(Based on work with Yuri Kovchegov and Huachen Sun, arXiv:2311.12208)

Probing gluon saturation with novel ratio R_{UPC} in ultra-peripheral collisions

Kong Tu (BNL)

Heavy nuclei at high energy are strongly modified

- ➢ EMC effect at large x
- ➢ Nuclear enhancement (anti-shadowing) at intermediate x
- ➢ Nuclear suppression at low x

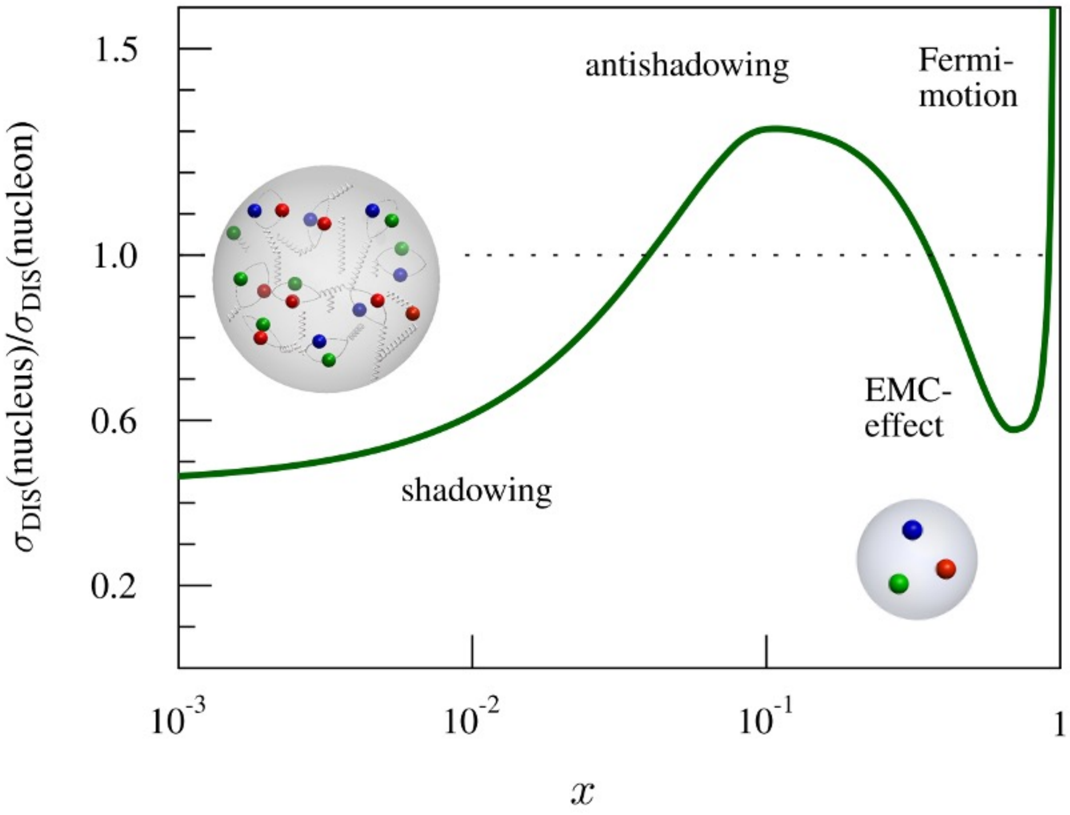

Heavy nuclei at high energy are strongly modified

- EMC effect at large x
- Nuclear enhancement (anti-shadowing) at intermediate x
- Nuclear suppression at low x

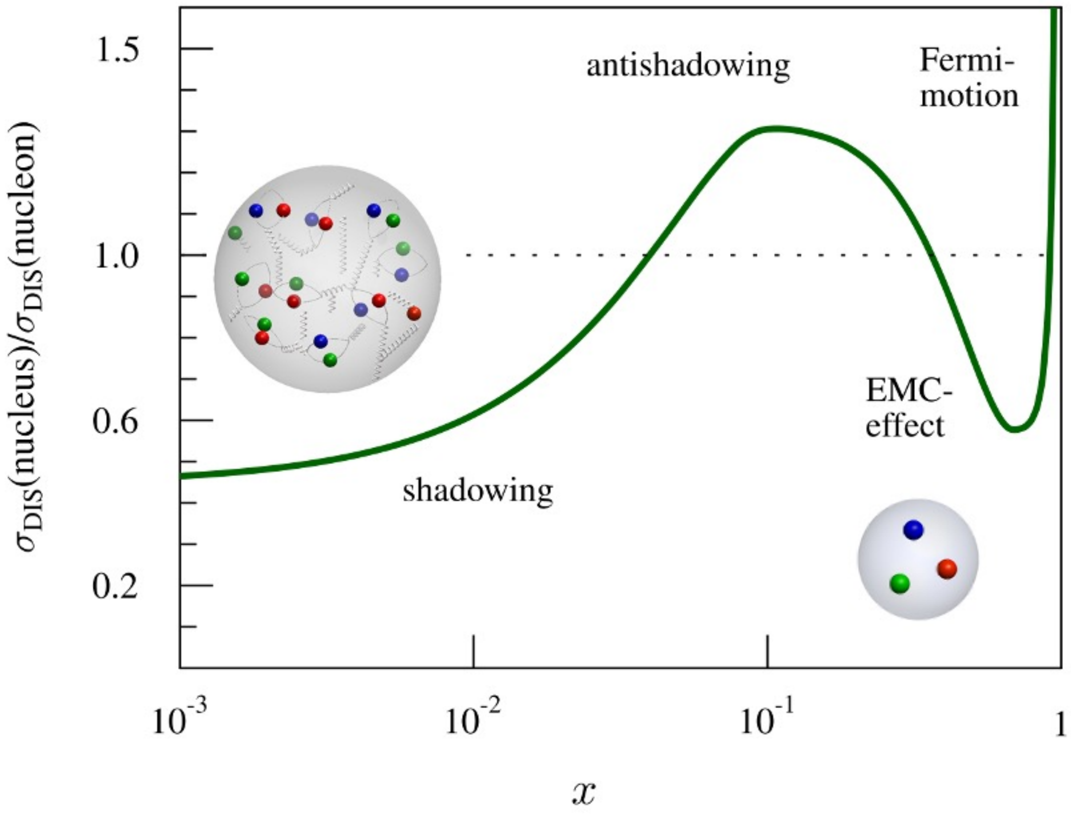

We know they exist, but we do not know (for sure) their underlying mechanisms.

Heavy nuclei at high energy are strongly modified

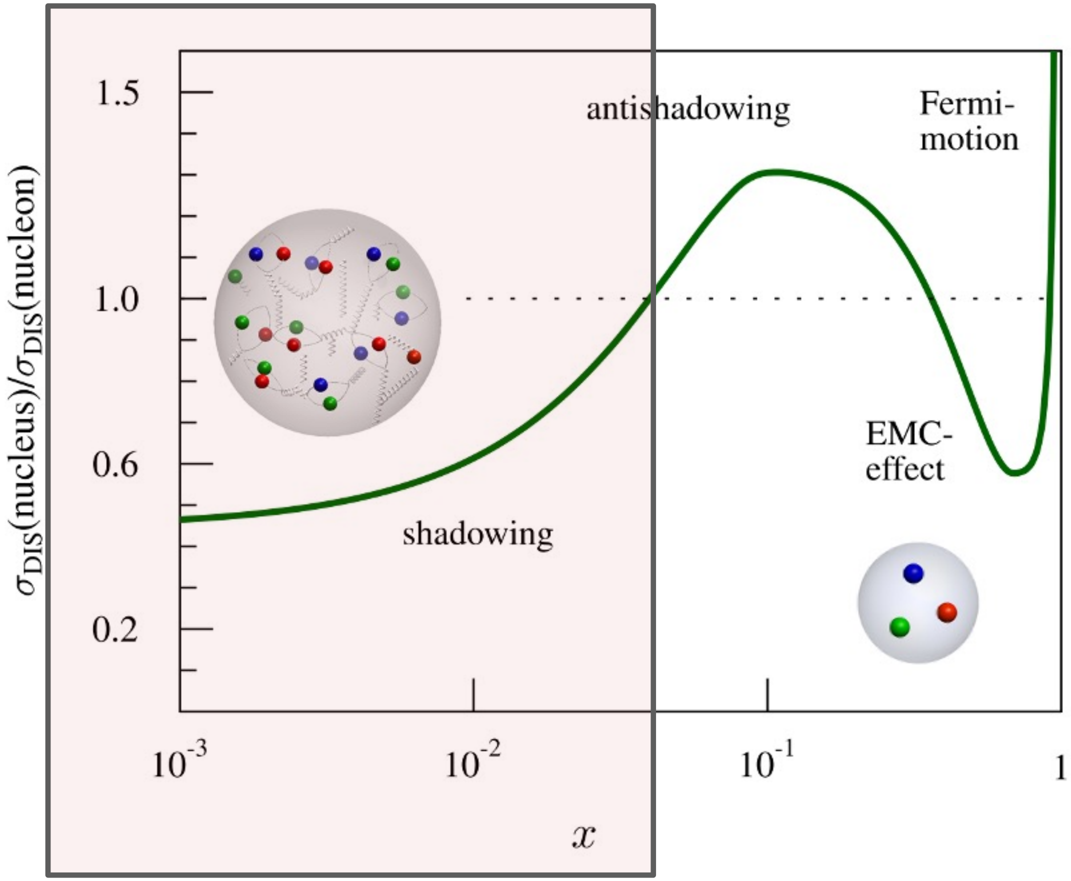

In this talk, I will focus on a **new measurement** that may find out the underlying mechanism at low-x.

Saturation of gluon density at high energy is expected

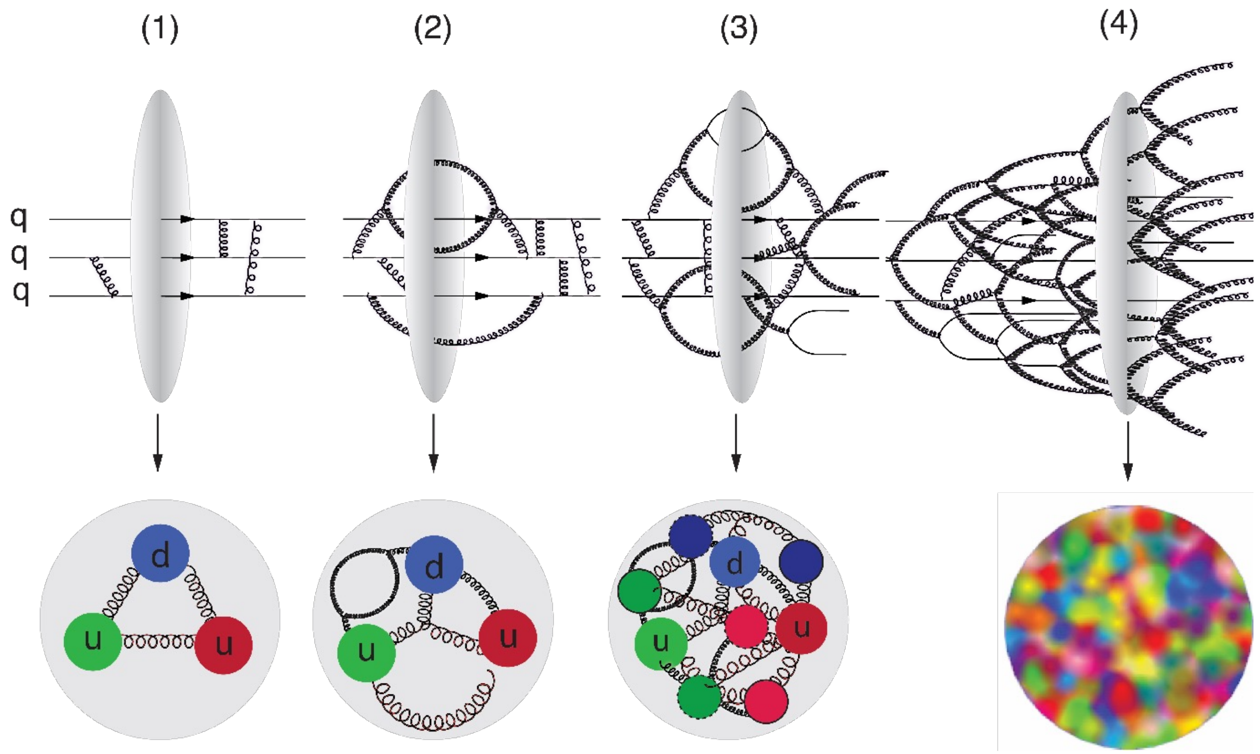

Saturation of gluon density at high energy is expected

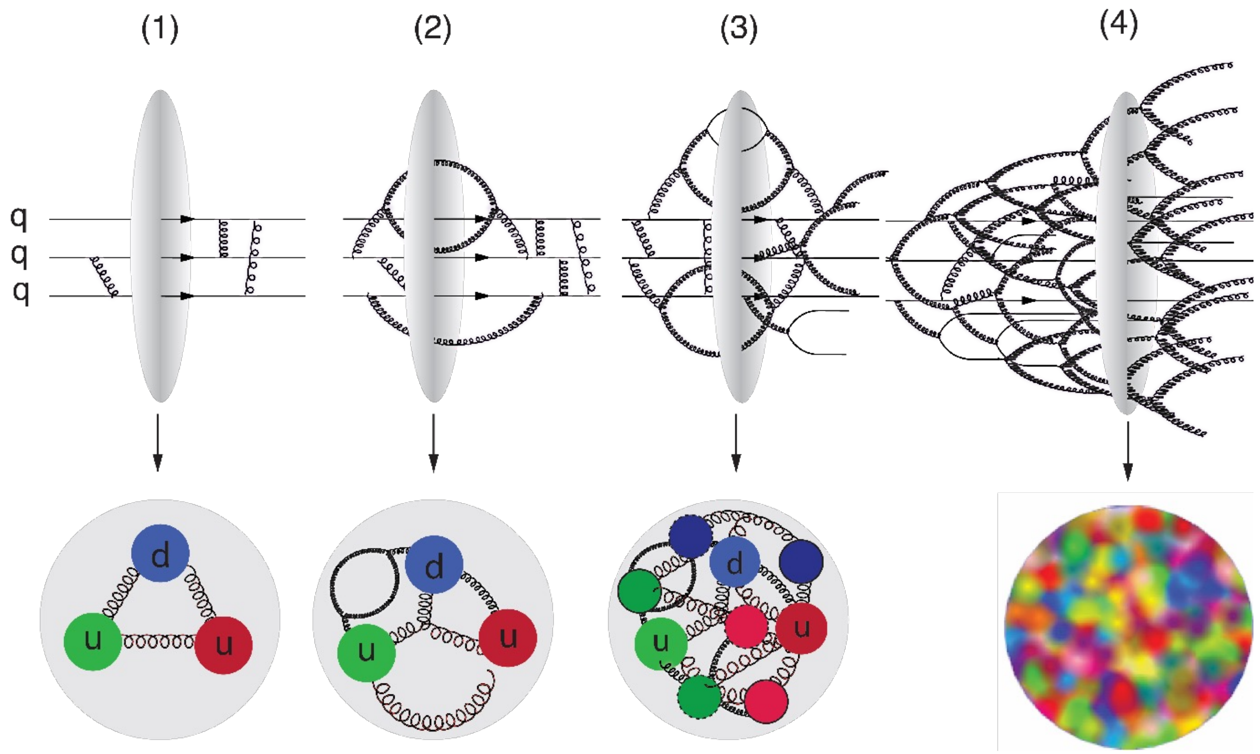

Saturation is a nonlinear gluon dynamics that gluon splitting ~ gluon recombination → **Therefore, it is a low-x phenomenon.**

(See details in other talks in this WG.)

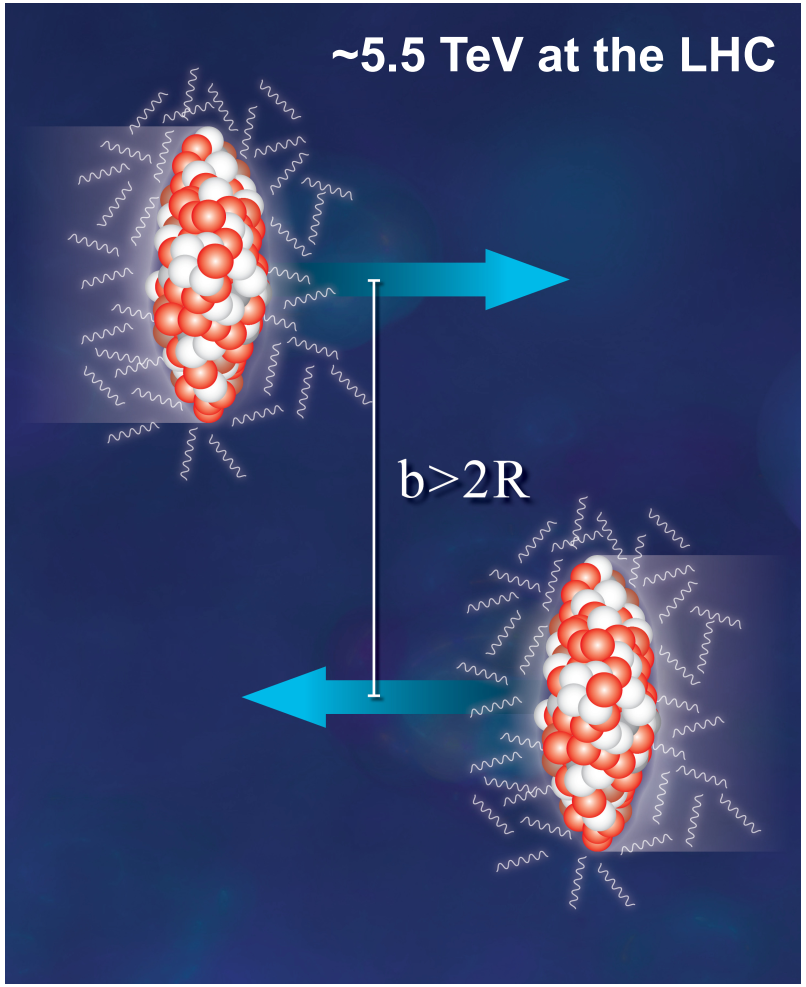

Vector Meson photoproduction in heavy-ion ultra-peripheral collisions (UPCs)

At Leading Order, 2-gluon exchange

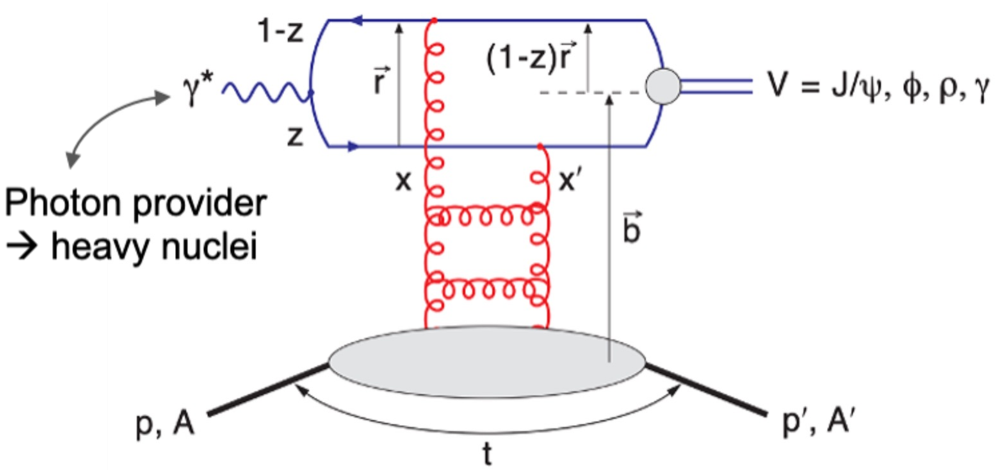

Coherent = nuclei stay intact
Incoherent = nuclei break up

A clean probe to the gluon density and gluon spatial distribution

Large nuclear suppression (even) up to x ~ 0.03

New

arXiv:2311.13637

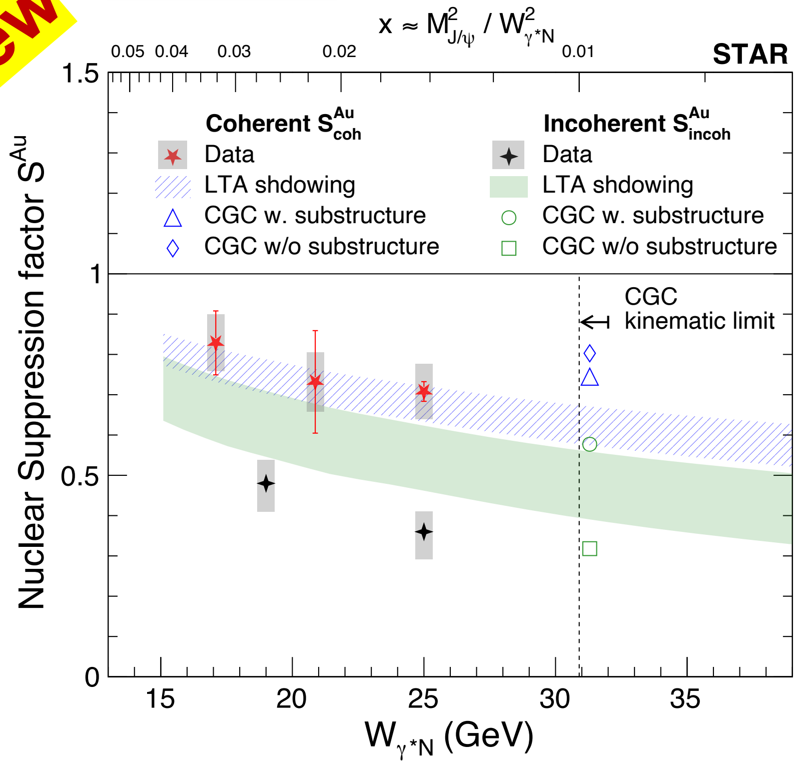

Relative to free nucleons
(Impulse Approximation)

Nuclear suppression was observed for both coherent and incoherent **J/ψ photoproduction at RHIC, with incoherent being more suppressed.**

Large nuclear suppression (even) up to x ~ 0.03

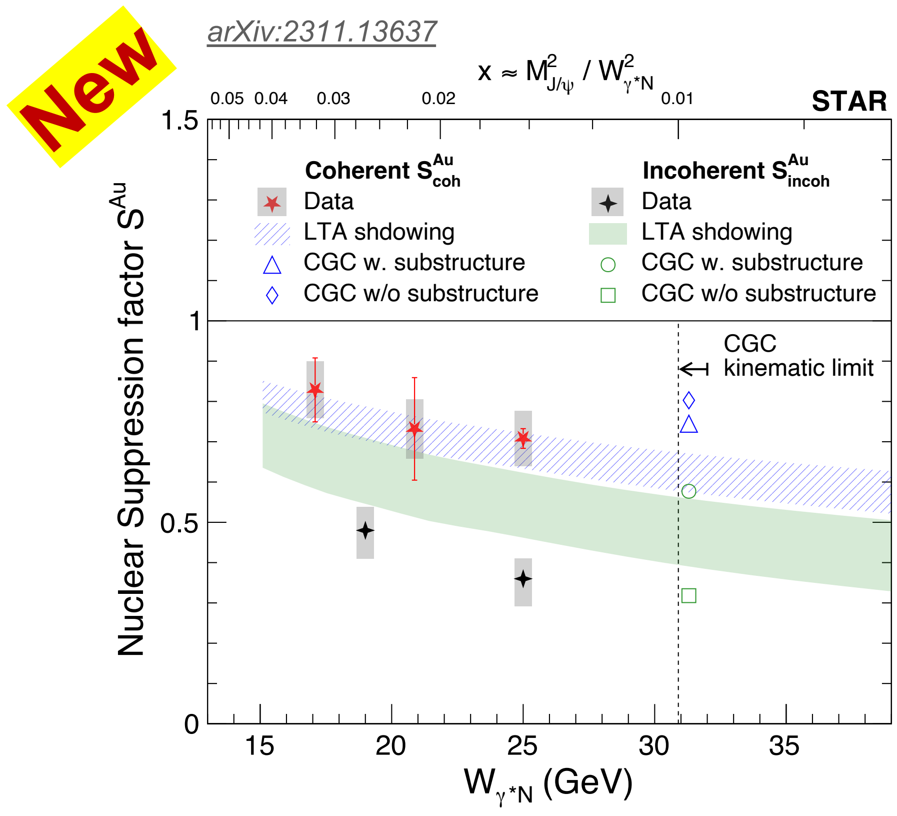

Relative to free nucleons
(Impulse Approximation)

Nuclear suppression was observed for both coherent and incoherent **J/ψ photoproduction at RHIC, with incoherent being more suppressed.**

- CGC **saturation** model, technically, has the limitation at the STAR's kinematics and data do not favor additional substructure with gluon density fluctuation.

Large nuclear suppression (even) up to x ~ 0.03

New

arXiv:2311.13637

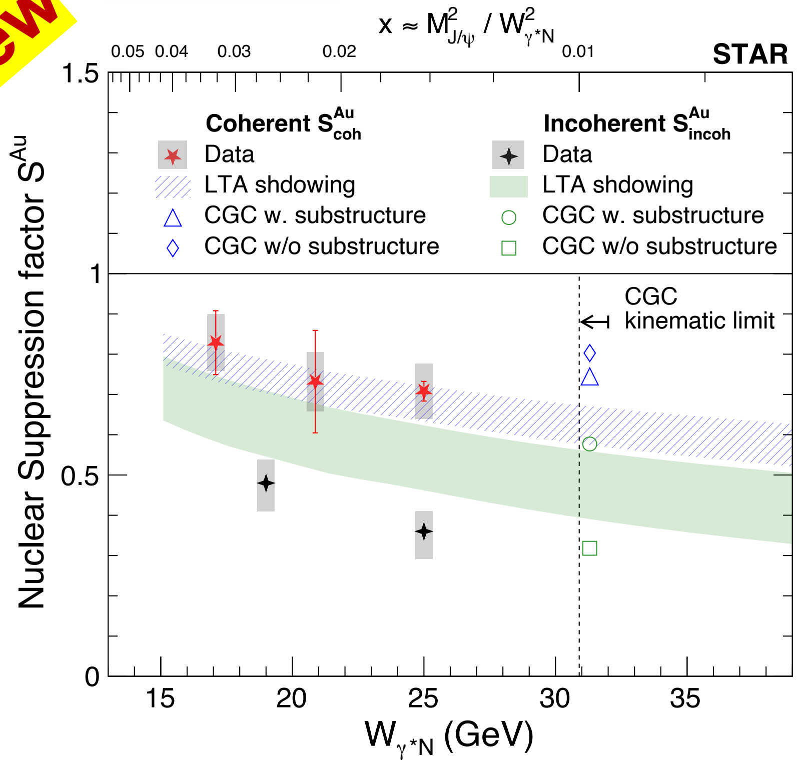

Relative to free nucleons
(Impulse Approximation)

Nuclear suppression was observed for both coherent and incoherent **J/ψ photoproduction at RHIC, with incoherent being more suppressed.**

- CGC **saturation** model, technically, has the limitation at the STAR's kinematics and data do not favor additional substructure with gluon density fluctuation.
- LTA in **nuclear shadowing** model describes the coherent well, but not enough suppression for incoherent production.

Leading Twist Approximation in nuclear shadowing

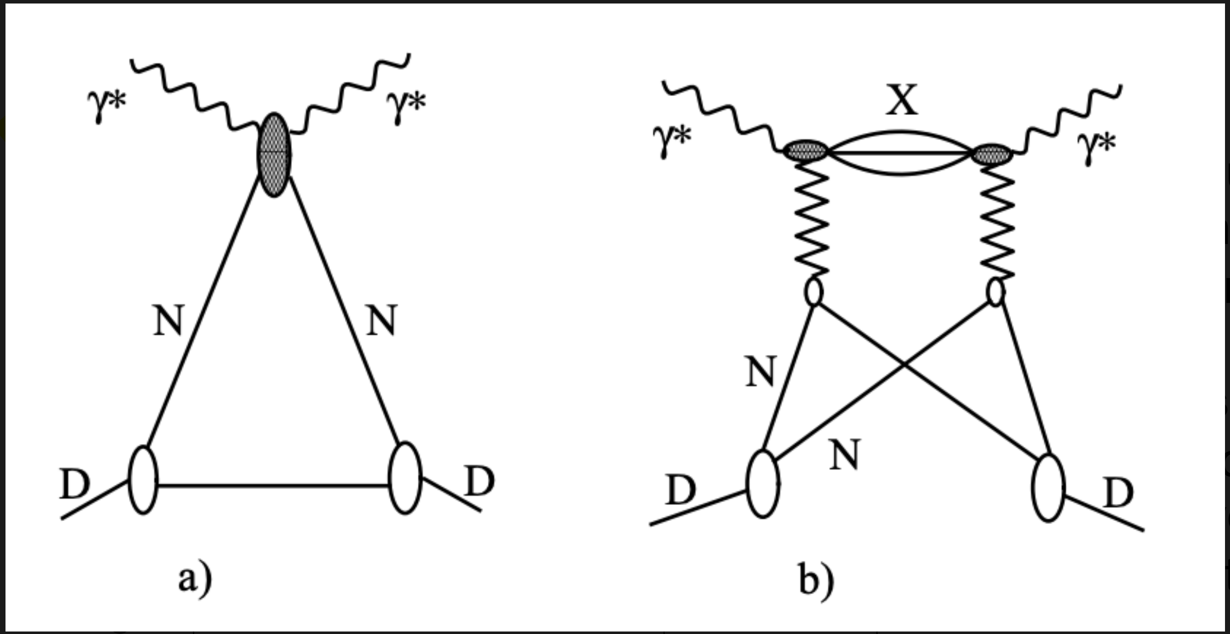

L. Frankfrut,, V. Guzey, M. Strikman (Physics Reports 512 (2012) 255-393)

Leading Twist Approximation (LTA)
Combination of Gribov-Glauber theory, QCD factorization, and HERA diffractive data

May not be exclusive to saturation, but certainly not identical. For example, proton target has no shadowing.

Large nuclear suppression down to x ~ 10^{-5}

PRL 131 (2023) 262301

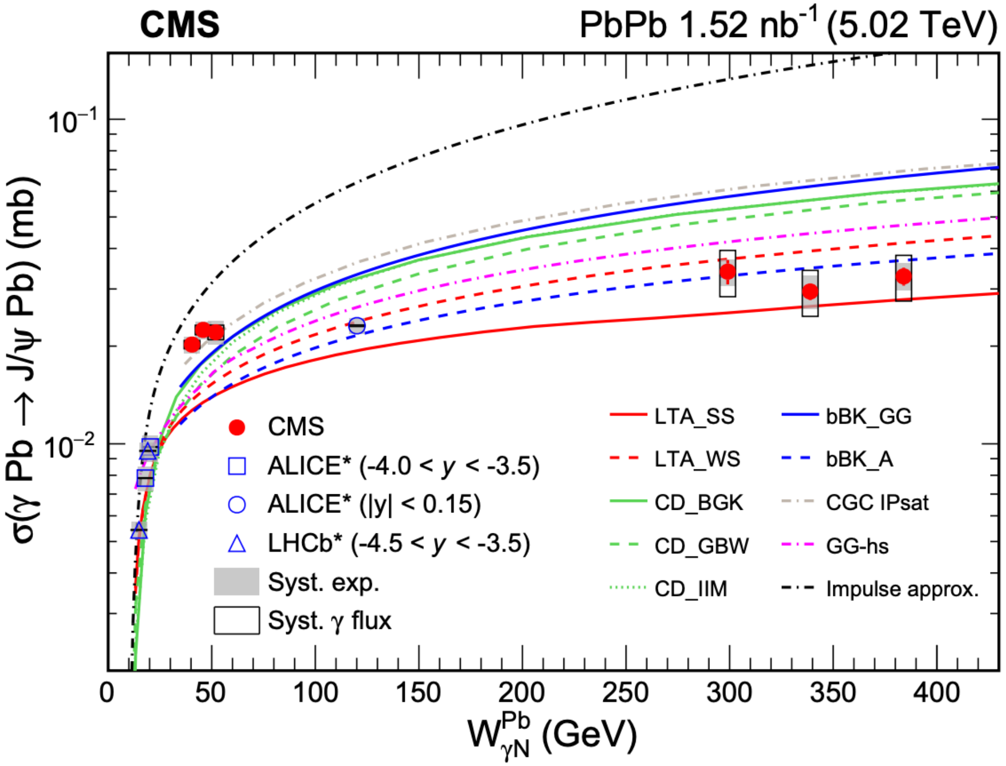

JHEP 10 (2023) 119

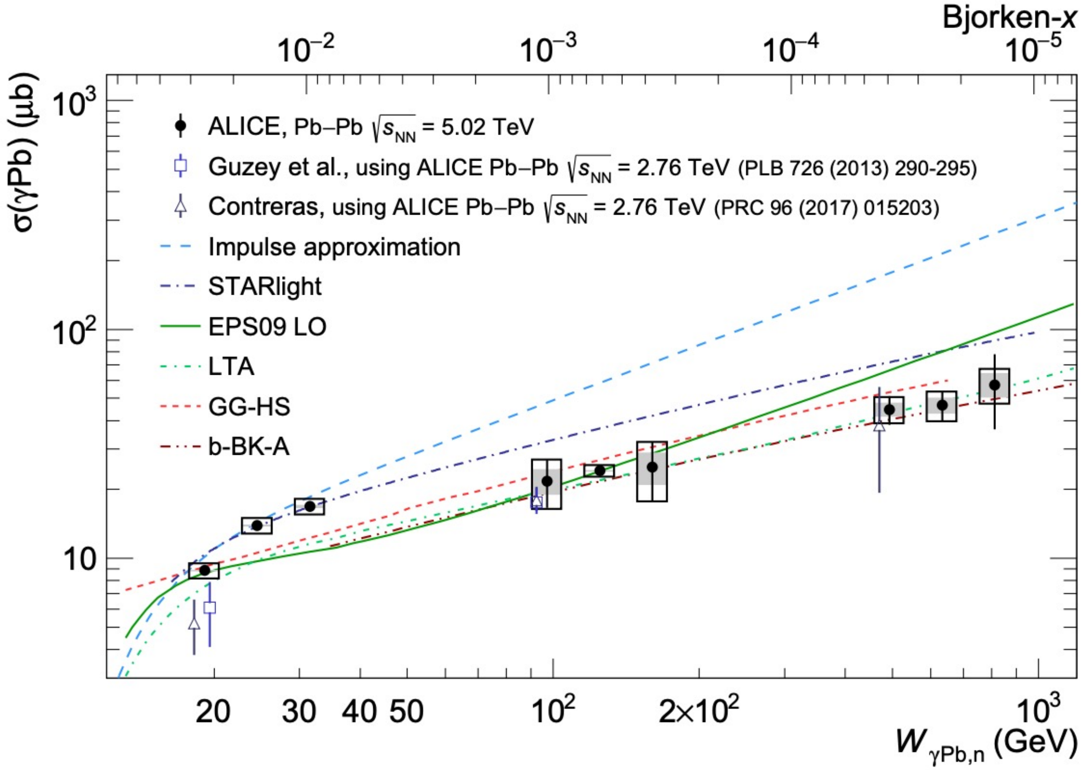

Both LTA shadowing models and saturation models can somewhat describe the higher energies.

Large nuclear suppression down to x ~ 10^{-5}

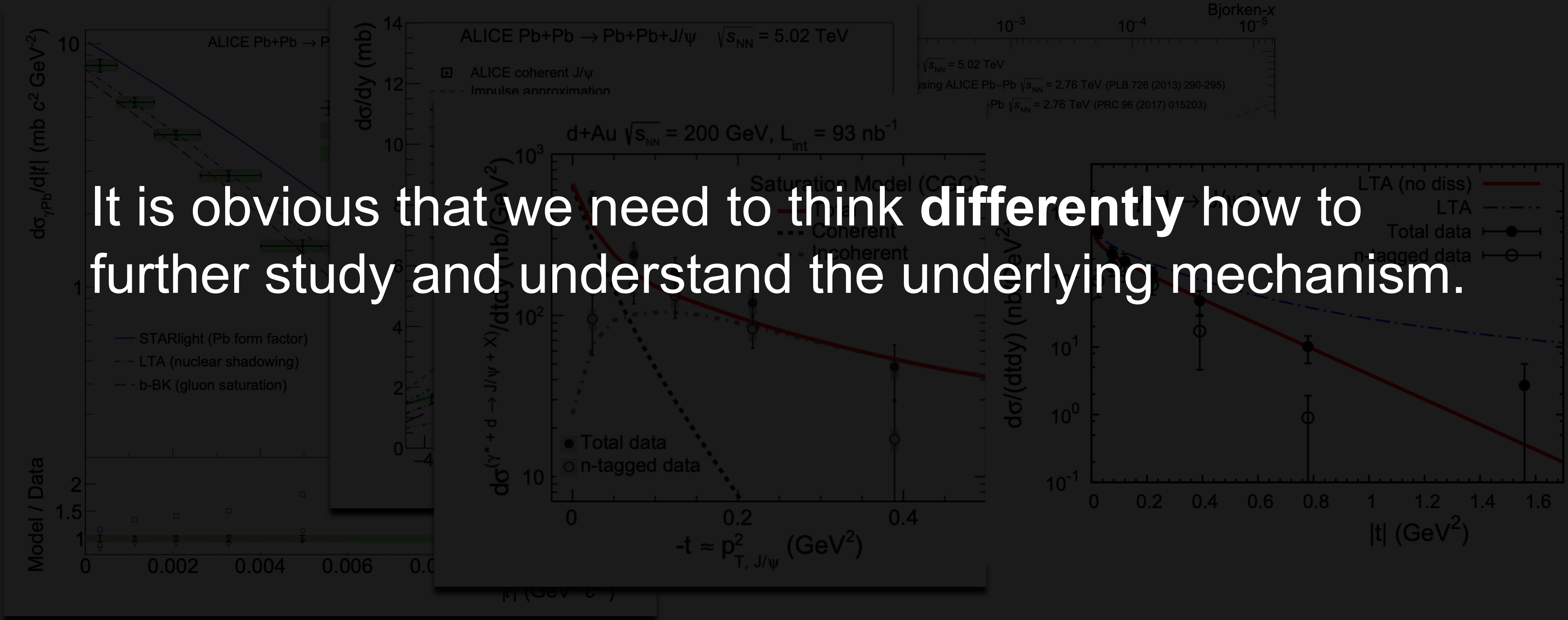

It is obvious that we need to think **differently** how to further study and understand the underlying mechanism.

A new proposal: double ratio in UPCs

$$R_{\mathrm{UPC}} = \frac{\left[\sigma_{\mathrm{el}}^{\mathrm{VM}} / \left(\mathrm{d}\sigma_{\mathrm{inclusive}}^{\mathrm{hadron/jet}} / \mathrm{d}^2 \mathrm{p_T}\right)\right]_{\gamma \mathrm{A}}}{\left[\sigma_{\mathrm{el}}^{\mathrm{VM}} / \left(\mathrm{d}\sigma_{\mathrm{inclusive}}^{\mathrm{hadron/jet}} / \mathrm{d}^2 \mathrm{p_T}\right)\right]_{\gamma \mathrm{p}}}$$

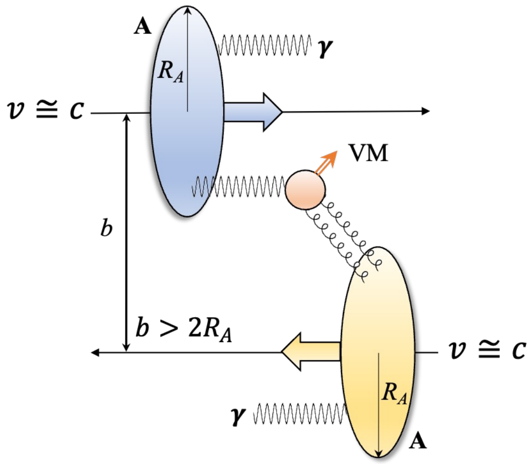

Vector Meson photoproduction

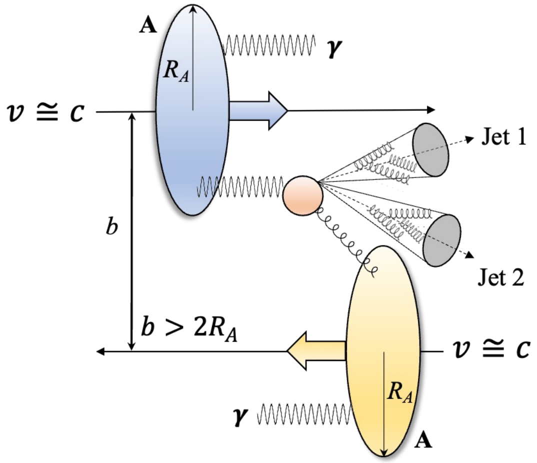

Jet photoproduction

A new proposal: double ratio in UPCs

$$R_{\mathrm{UPC}} = \frac{\left[\sigma_{\mathrm{el}}^{\mathrm{VM}} / \left(\mathrm{d}\sigma_{\mathrm{inclusive}}^{\mathrm{hadron/jet}} / \mathrm{d}^2 \mathrm{p_T}\right)\right]_{\gamma \mathrm{A}}}{\left[\sigma_{\mathrm{el}}^{\mathrm{VM}} / \left(\mathrm{d}\sigma_{\mathrm{inclusive}}^{\mathrm{hadron/jet}} / \mathrm{d}^2 \mathrm{p_T}\right)\right]_{\gamma \mathrm{p}}}$$

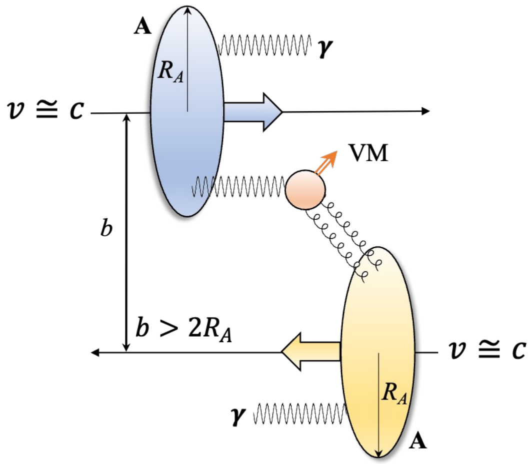

Vector Meson photoproduction

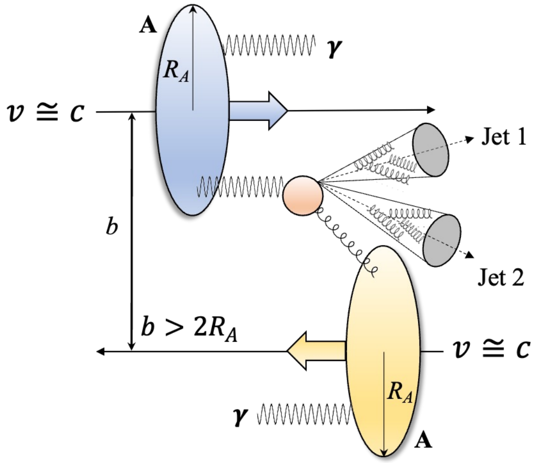

Jet photoproduction

Distinct expectation:

- Saturation: diffractive J/ψ is less suppressed than inclusive jet/*h* production.
- Shadowing: diffractive J/ψ is more suppressed than inclusive jet/*h* production

CGC: calculating the double ratio

$$R_{\mathrm{UPC}} = \frac{\left[\sigma_{\mathrm{el}}^{\mathrm{VM}} / \left(\mathrm{d}\sigma_{\mathrm{inclusive}}^{\mathrm{hadron/jet}} / \mathrm{d}^2 \mathrm{p_T}\right)\right]_{\gamma\mathrm{A}}}{\left[\sigma_{\mathrm{el}}^{\mathrm{VM}} / \left(\mathrm{d}\sigma_{\mathrm{inclusive}}^{\mathrm{hadron/jet}} / \mathrm{d}^2 \mathrm{p_T}\right)\right]_{\gamma\mathrm{p}}}$$

CGC: calculating the double ratio – Vector Meson (VM)

$$R_{\mathrm{UPC}} = \frac{\left[\boxed{\sigma_{\mathrm{el}}^{\mathrm{VM}}} / \left(\mathrm{d}\sigma_{\mathrm{inclusive}}^{\mathrm{hadron/jet}} / \mathrm{d}^2\mathrm{p_T}\right)\right]_{\gamma\mathrm{A}}}{\left[\sigma_{\mathrm{el}}^{\mathrm{VM}} / \left(\mathrm{d}\sigma_{\mathrm{inclusive}}^{\mathrm{hadron/jet}} / \mathrm{d}^2\mathrm{p_T}\right)\right]_{\gamma\mathrm{p}}}$$

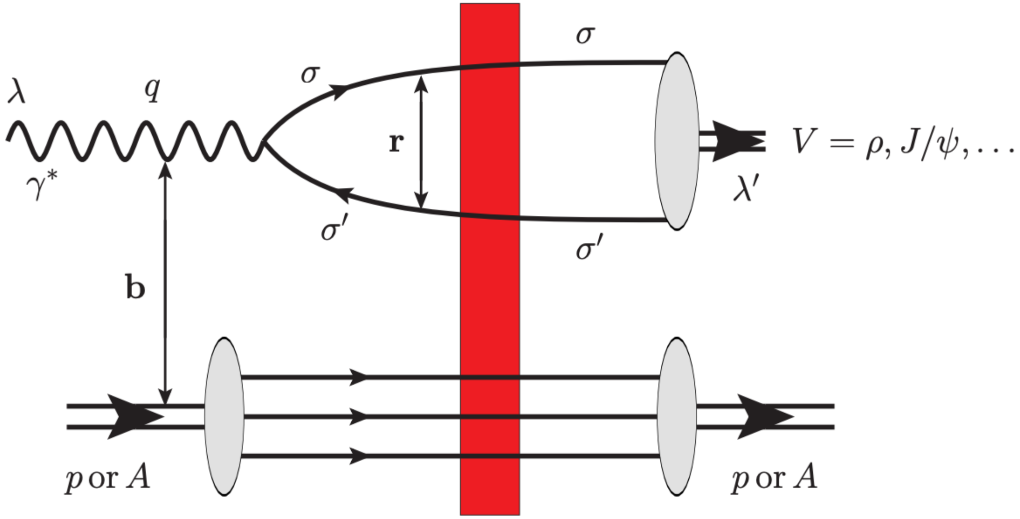

Standard CGC framework, dipole amplitude from BK/JIMWLK, GGM/MV model for initial condition, etc.

Two knobs to turn: the target and the probe

A

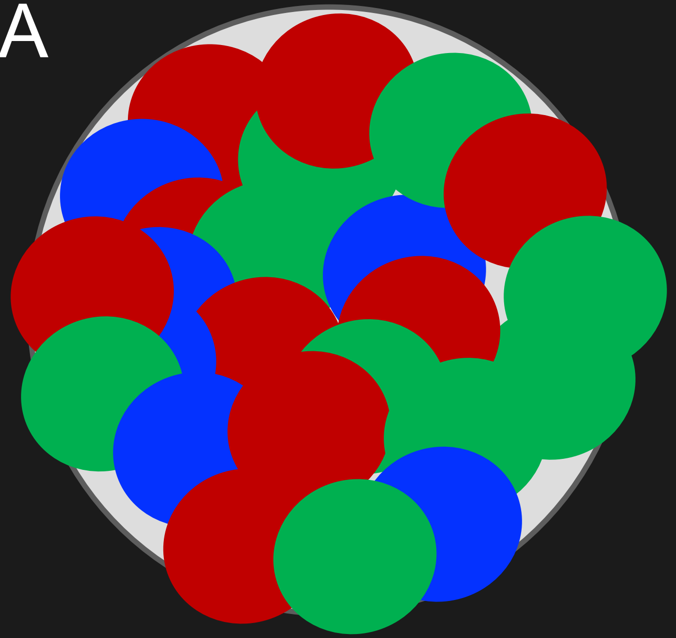

$1/Q_s$ vs r = dipole size

High energy

$Q_s^2 \sim (A/x)^{1/3}$

Target

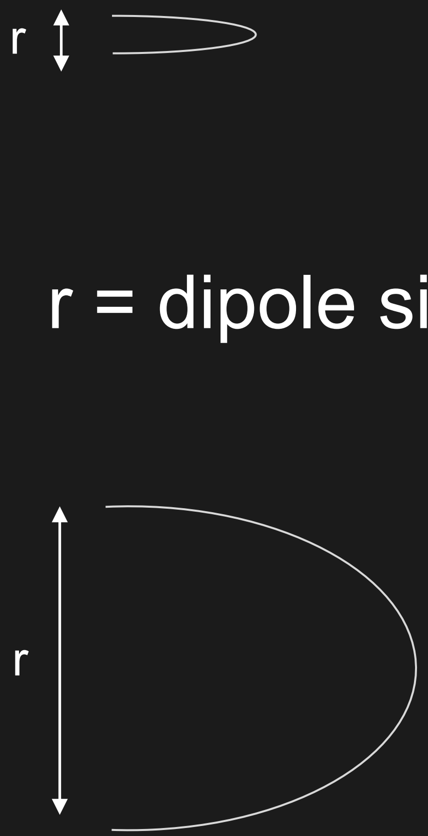

Non-saturation

Saturation

Probe

CGC: A-scaling for J/ψ and ρ meson

$$R_{\mathrm{UPC}} = \frac{\left[\boxed{\sigma_{\mathrm{el}}^{\mathrm{VM}}} / \left(\mathrm{d}\sigma_{\mathrm{inclusive}}^{\mathrm{hadron/jet}} / \mathrm{d}^2\mathrm{p_T}\right)\right]_{\gamma\mathrm{A}}}{\left[\sigma_{\mathrm{el}}^{\mathrm{VM}} / \left(\mathrm{d}\sigma_{\mathrm{inclusive}}^{\mathrm{hadron/jet}} / \mathrm{d}^2\mathrm{p_T}\right)\right]_{\gamma\mathrm{p}}}$$

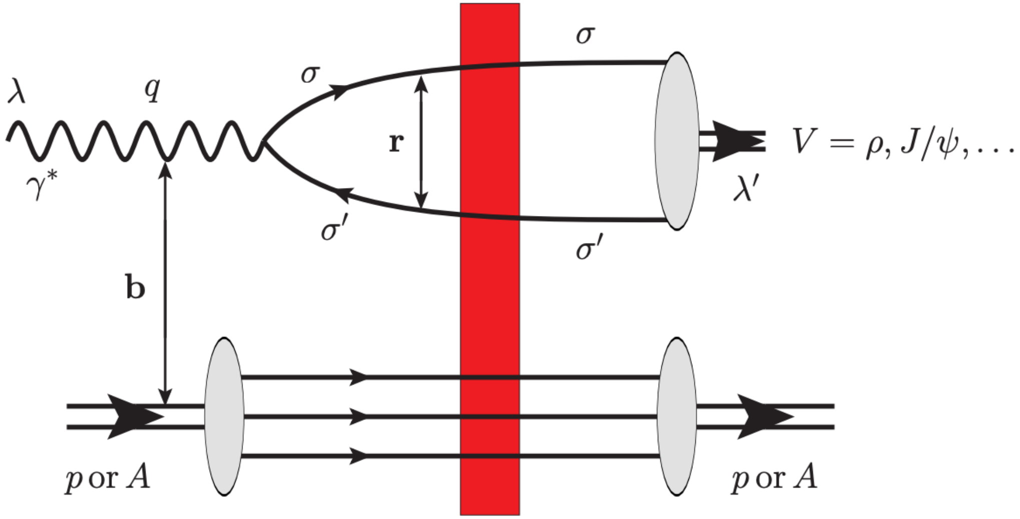

Standard CGC framework, dipole amplitude from BK/JIMWLK, GGM/MV model for initial condition, etc

$$\sigma_{\mathrm{el}}^{\gamma^* \mathrm{A} \to V \mathrm{A}} \propto \begin{cases} A^{4/3}, & \text{outside the saturation region,} \\ A^{2/3}, & \text{inside the saturation region.} \end{cases}$$

J/ψ

ρ

CGC: calculating the double ratio – inclusive quark

$$R_{\mathrm{UPC}} = \frac{\left[\sigma_{\mathrm{el}}^{\mathrm{VM}} / \boxed{\left(\mathrm{d}\sigma_{\mathrm{inclusive}}^{\mathrm{hadron/jet}} / \mathrm{d}^2\mathrm{p_T}\right)}\right]_{\gamma\mathrm{A}}}{\left[\sigma_{\mathrm{el}}^{\mathrm{VM}} / \left(\mathrm{d}\sigma_{\mathrm{inclusive}}^{\mathrm{hadron/jet}} / \mathrm{d}^2\mathrm{p_T}\right)\right]_{\gamma\mathrm{p}}}$$

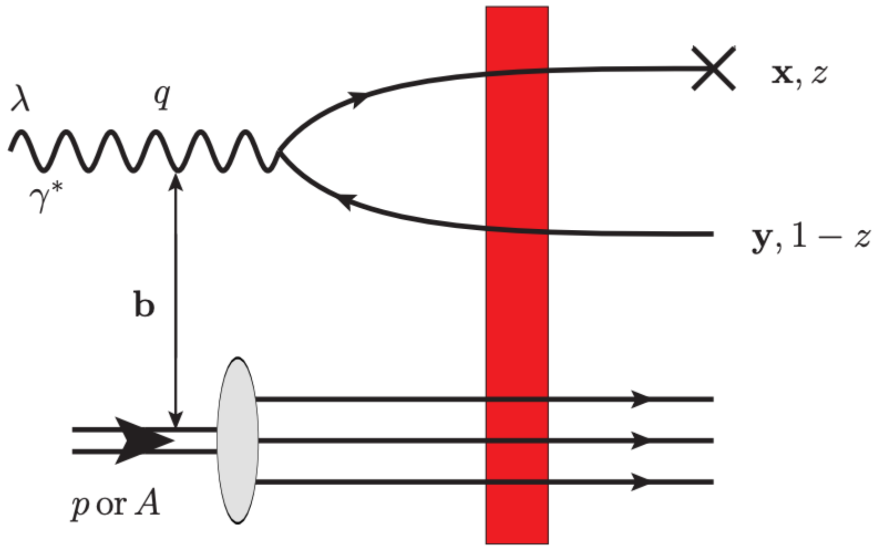

Similar calculations, except quark-antiquark pair doesn't become VM, target breaks up so no color-singlet, etc. **"X" is the measured parton.**

CGC: calculating the double ratio – inclusive quark

$$R_{\mathrm{UPC}} = \frac{\left[\sigma_{\mathrm{el}}^{\mathrm{VM}} / \boxed{\left(\mathrm{d}\sigma_{\mathrm{inclusive}}^{\mathrm{hadron/jet}} / \mathrm{d}^2 \mathrm{p_T}\right)}\right]_{\gamma\mathrm{A}}}{\left[\sigma_{\mathrm{el}}^{\mathrm{VM}} / \left(\mathrm{d}\sigma_{\mathrm{inclusive}}^{\mathrm{hadron/jet}} / \mathrm{d}^2 \mathrm{p_T}\right)\right]_{\gamma\mathrm{p}}}$$

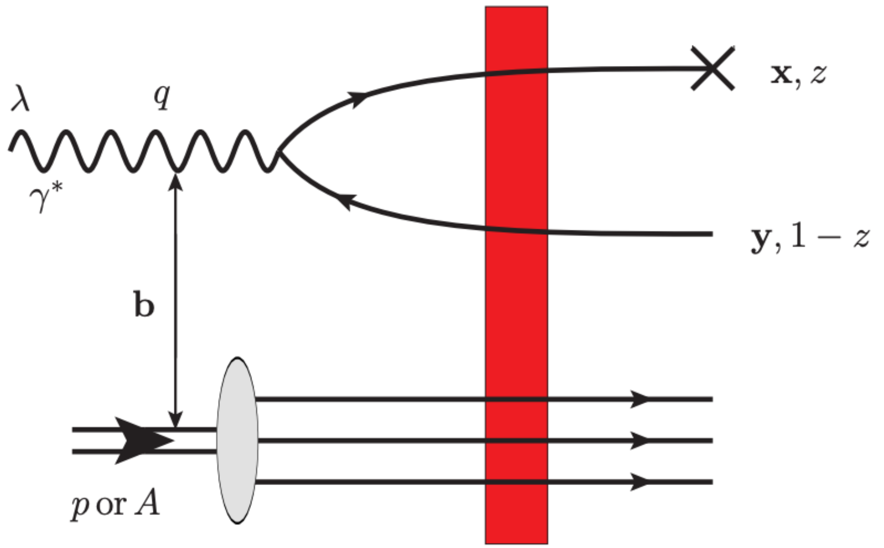

Similar calculations, except quark-antiquark pair doesn't become VM, target breaks up so no color-singlet, etc. **"X" is the measured parton.**

$$\boxed{\frac{d\sigma}{d^2 p_T} \propto \begin{cases} A, & p_T \gg Q_s\,, \\ A^{2/3}, & p_T \ll Q_s\,. \end{cases}}$$

CGC: A-scaling for J/ψ and ρ meson

$$R_{\mathrm{UPC}} = \boxed{\frac{\left[\sigma_{\mathrm{el}}^{\mathrm{VM}} / \left(\mathrm{d}\sigma_{\mathrm{inclusive}}^{\mathrm{hadron/jet}} / \mathrm{d}^2 \mathrm{p_T}\right)\right]_{\gamma \mathrm{A}}}{\left[\sigma_{\mathrm{el}}^{\mathrm{VM}} / \left(\mathrm{d}\sigma_{\mathrm{inclusive}}^{\mathrm{hadron/jet}} / \mathrm{d}^2 \mathrm{p_T}\right)\right]_{\gamma \mathrm{p}}}}$$

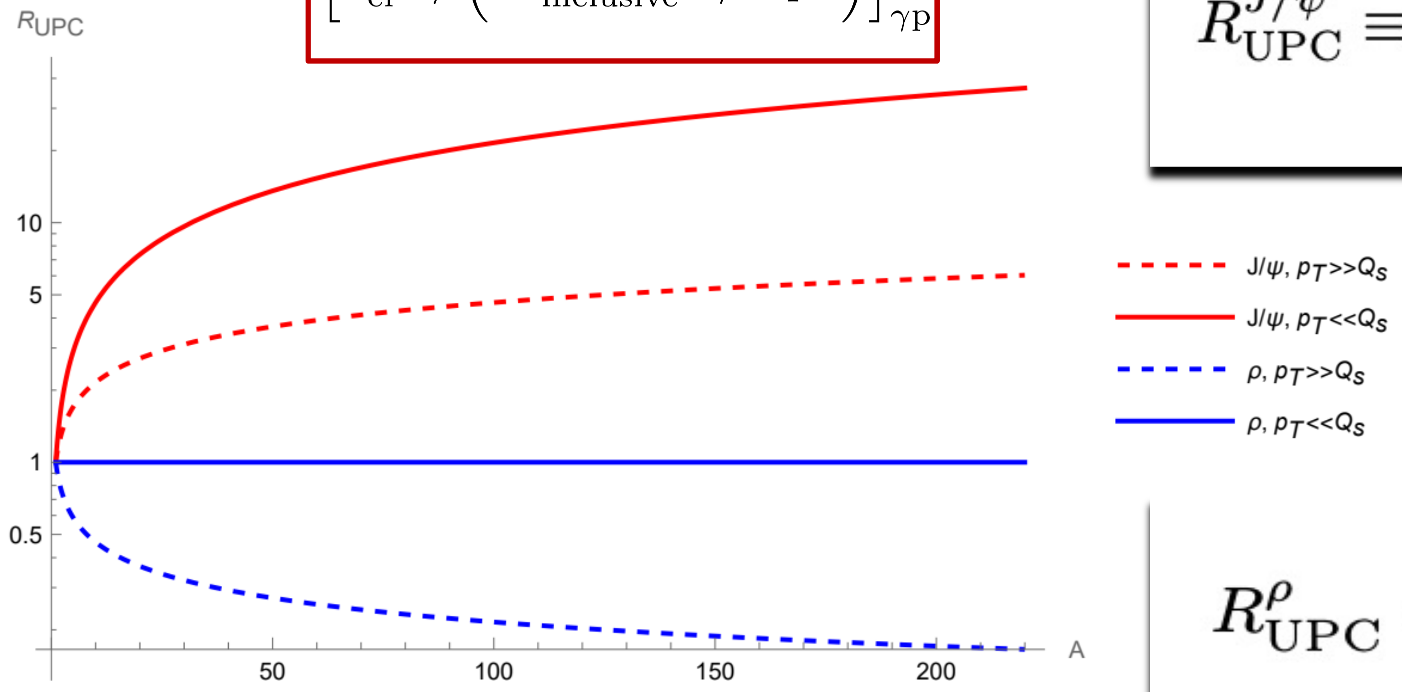

$$R_{\mathrm{UPC}}^{J/\psi} \equiv \frac{R_1^{J/\psi}(\mathrm{A})}{R_1^{J/\psi}(p)} = \begin{cases} A^{\frac{1}{3}}, & p_T \gg Q_s, \\ A^{\frac{2}{3}}, & p_T \ll Q_s. \end{cases}$$

$$R_{\mathrm{UPC}}^{\rho} = \begin{cases} A^{-\frac{1}{3}}, & p_T \gg Q_s, \\ A^0 = 1, & p_T \ll Q_s. \end{cases}$$

Shadowing model prediction for R_{UPC}?

$$R_{\mathrm{UPC}} = \frac{\left[\sigma_{\mathrm{el}}^{\mathrm{VM}} / \left(\mathrm{d}\sigma_{\mathrm{inclusive}}^{\mathrm{hadron/jet}} / \mathrm{d}^2 \mathrm{p_T}\right)\right]_{\gamma \mathrm{A}}}{\left[\sigma_{\mathrm{el}}^{\mathrm{VM}} / \left(\mathrm{d}\sigma_{\mathrm{inclusive}}^{\mathrm{hadron/jet}} / \mathrm{d}^2 \mathrm{p_T}\right)\right]_{\gamma \mathrm{p}}}$$

Claim: this double ratio may provide the maximal separation between the two models

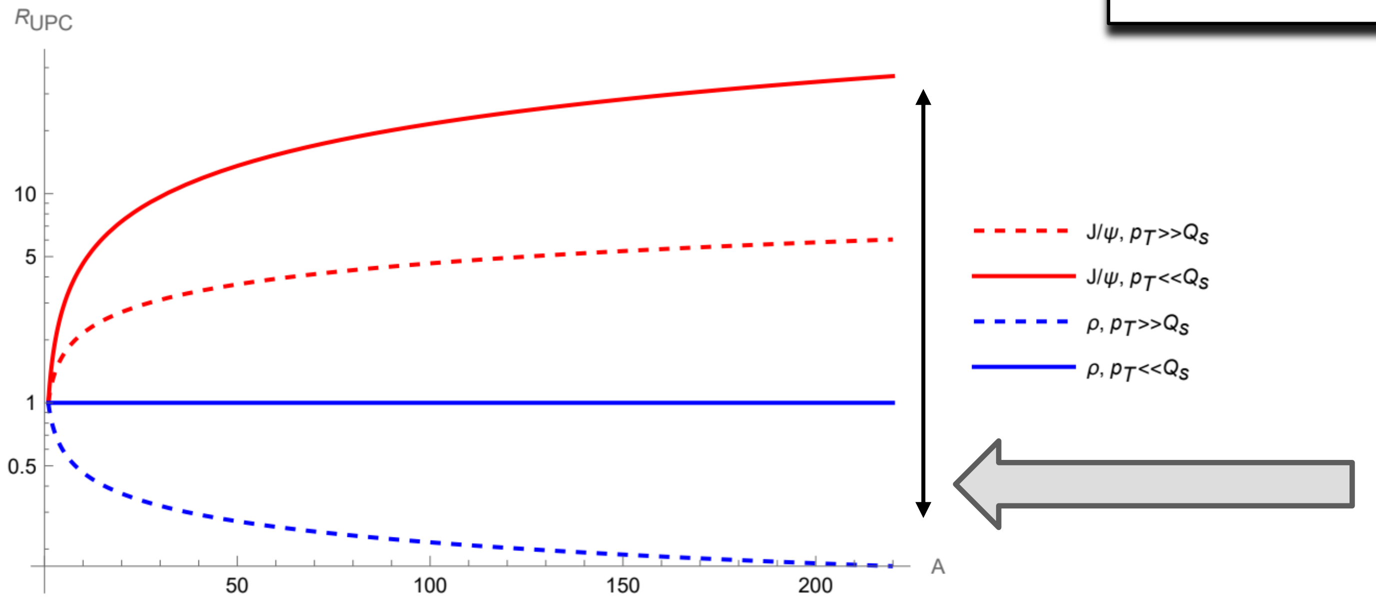

My naïve expectation would be somewhere here but need proper calculations.

Measurement at RHIC and the LHC

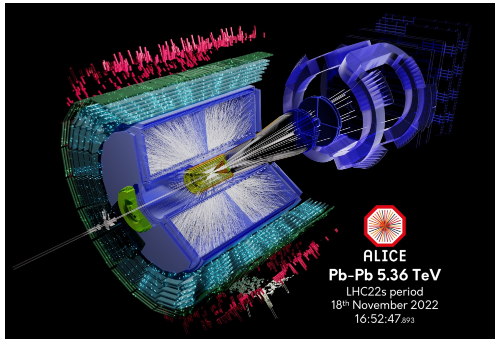

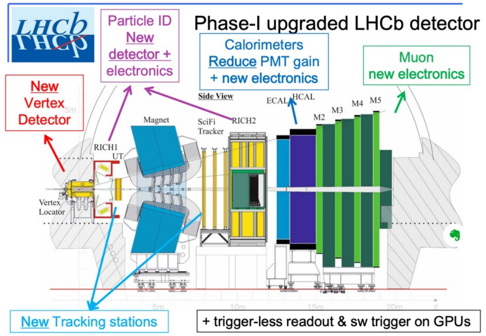

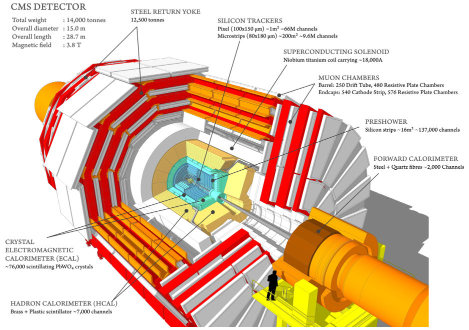

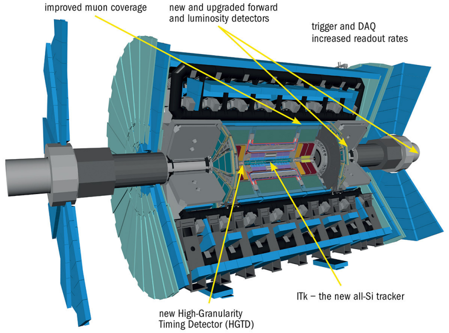

All LHC experiments will have significant upgrades in Run 3 & 4 (e.g., wide acceptances, ALICE FoCal, etc.). **Lower-x reach!**

Measurement at RHIC and the LHC

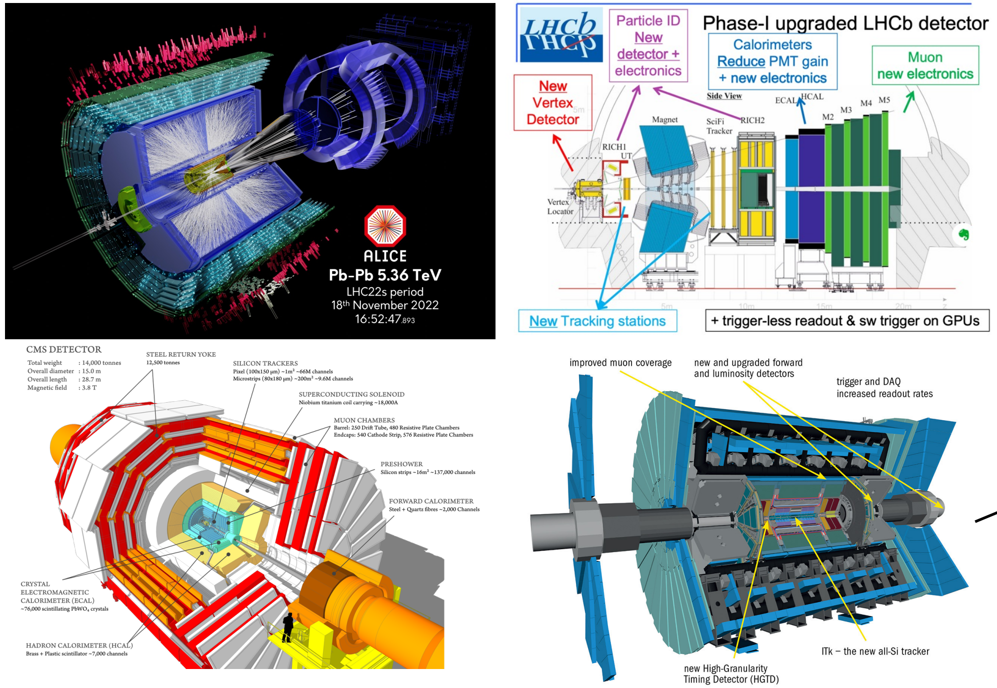

All LHC experiments will have significant upgrades in Run 3 & 4 (e.g., wide acceptances, ALICE FoCal, etc.). **Lower-x reach!**

ATLAS recently joined the game of UPC **J/ψ in Run 3**

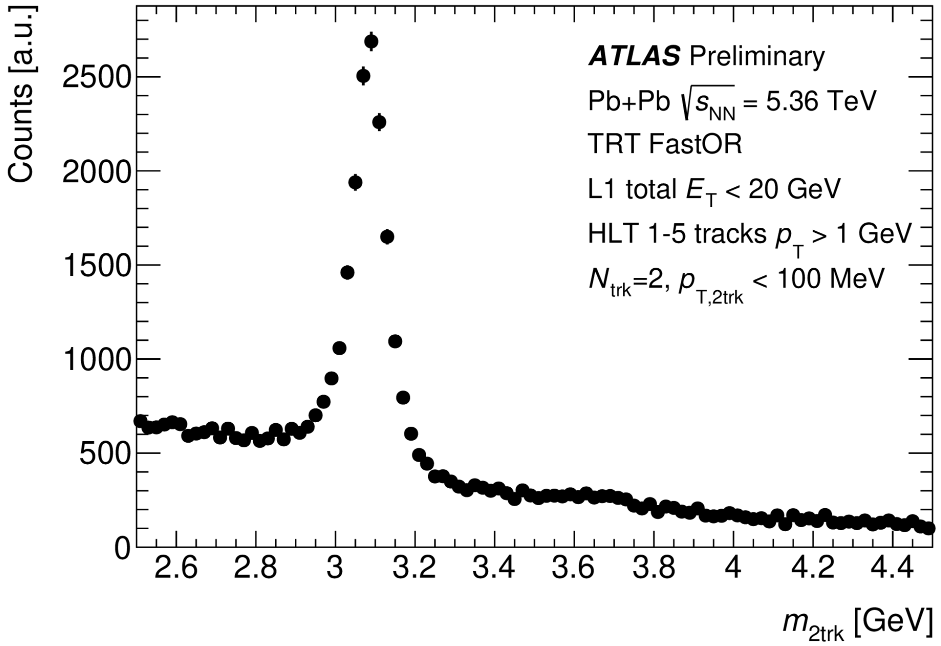

ATLAS had shown capabilities of doing jet/hadron in UPCs too.

Kong Tu

Connection to the Electron-Ion Collider

EIC

The ePIC detector and possible a 2nd detector

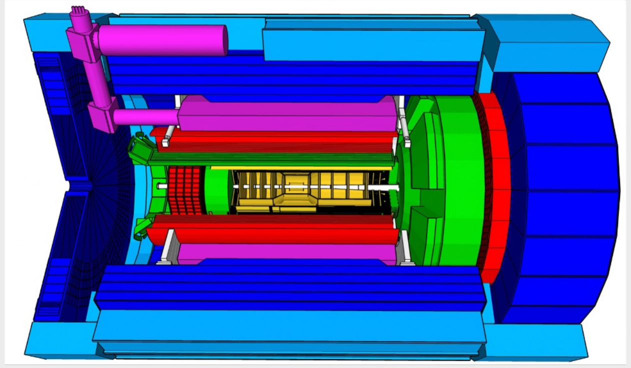

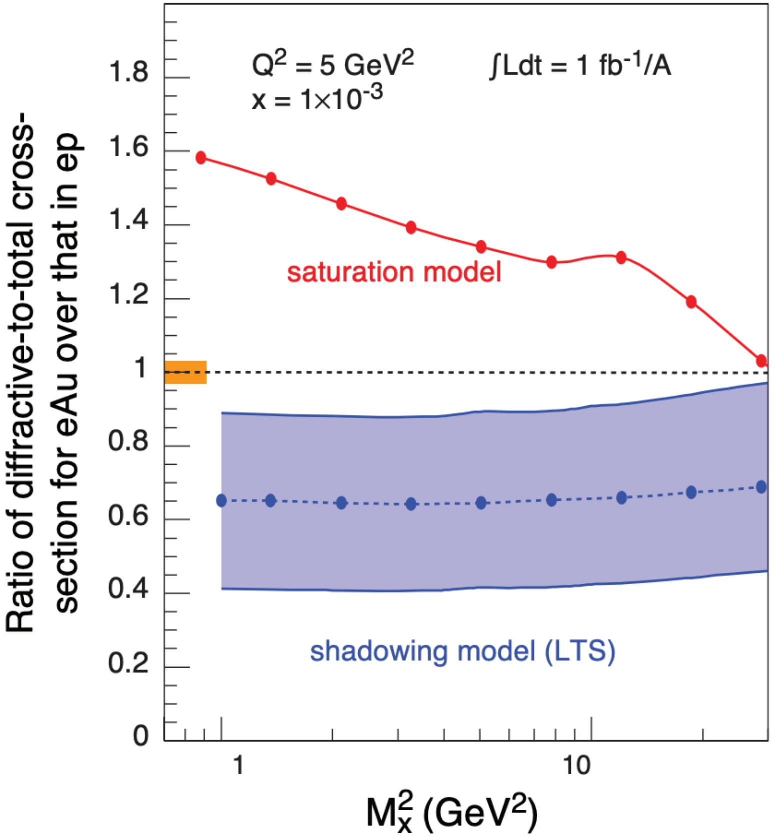

$$R_{\mathrm{EIC}} = \frac{\left[\left(d\sigma_{\mathrm{diff}}/dM_X^2\right)/\sigma_{\mathrm{tot}}\right]_{\mathrm{e+A}}}{\left[\left(d\sigma_{\mathrm{diff}}/dM_X^2\right)/\sigma_{\mathrm{tot}}\right]_{\mathrm{e+p}}},$$

Similar idea from the EIC white paper with diffractive DIS and total DIS cross section.

Summary: double ratio R_{UPC} for understanding the low-x nuclear suppression

- One of the most pressing questions in UPC VM measurements is to confirm or validate models.
- New observable $\mathbf{R_{UPC}}$ may shine new light to this question
- **RHIC and LHC** provide a wide range of energy to test R_{UPC} and may have a few different nuclei to see the *A* dependence.

$$R_{\rm UPC} = \frac{\left[\sigma_{\rm el}^{\rm VM} / \left({\rm d}\sigma_{\rm inclusive}^{\rm hadron/jet} / {\rm d}^2 {\rm p_T}\right)\right]_{\gamma {\rm A}}}{\left[\sigma_{\rm el}^{\rm VM} / \left({\rm d}\sigma_{\rm inclusive}^{\rm hadron/jet} / {\rm d}^2 {\rm p_T}\right)\right]_{\gamma {\rm p}}}$$

"*Every genuine test of a theory is an attempt to falsify it, or to refute it*" – Karl Popper.

Thank you!

Backup

Most, if not all, data and model comparisons are like these

PRL 131 (2023) 262301

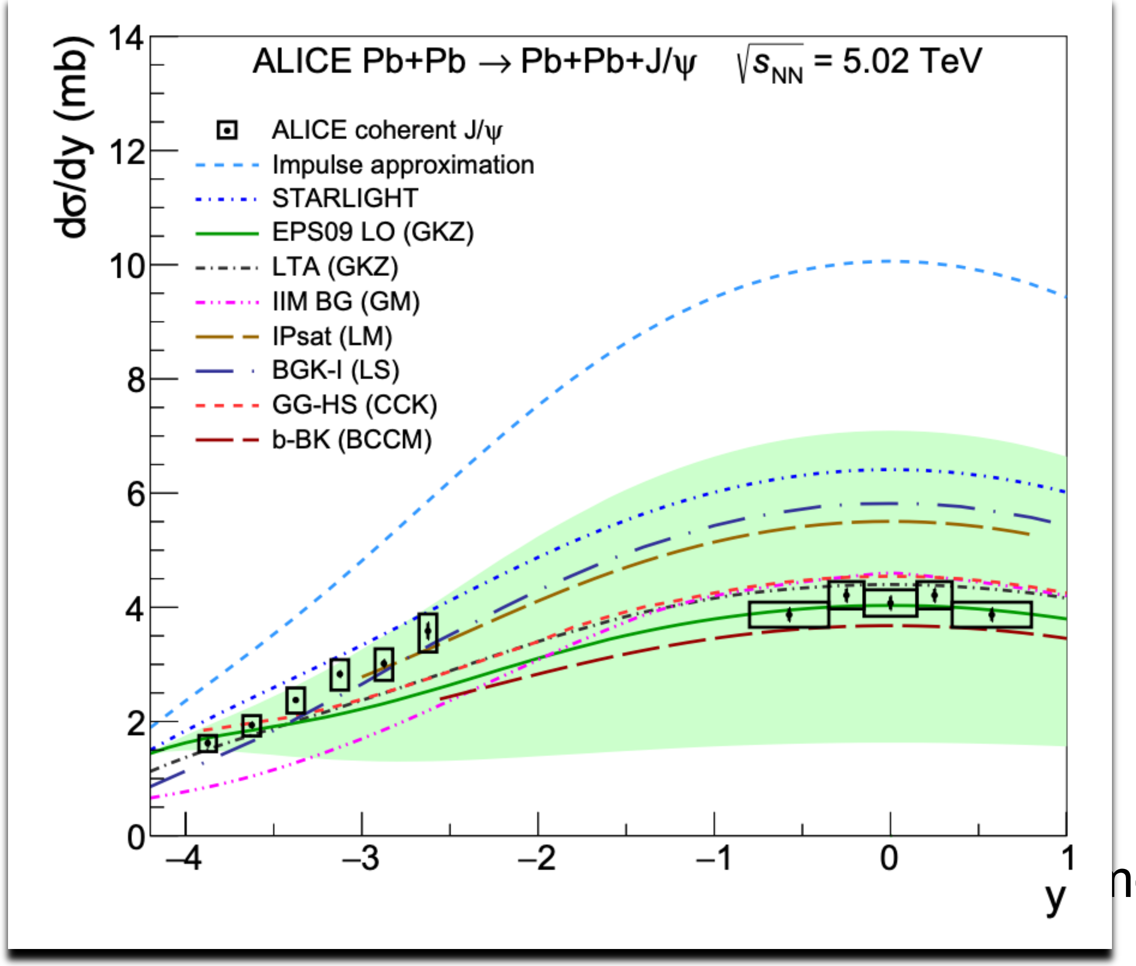

JHEP 10 (2023) 119

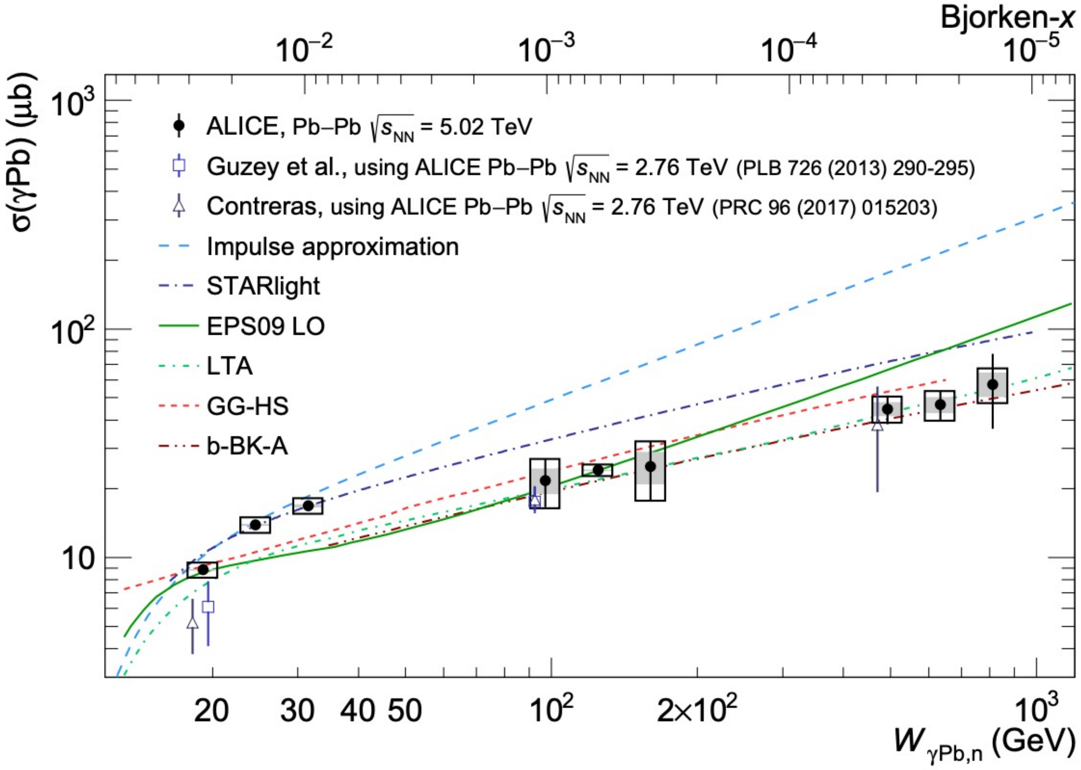

nodels can somewhat describe the higher energies.

Most, if not all, data and model comparisons are like these

PRL 131 (2023) 262301

JHEP 10 (2023) 119

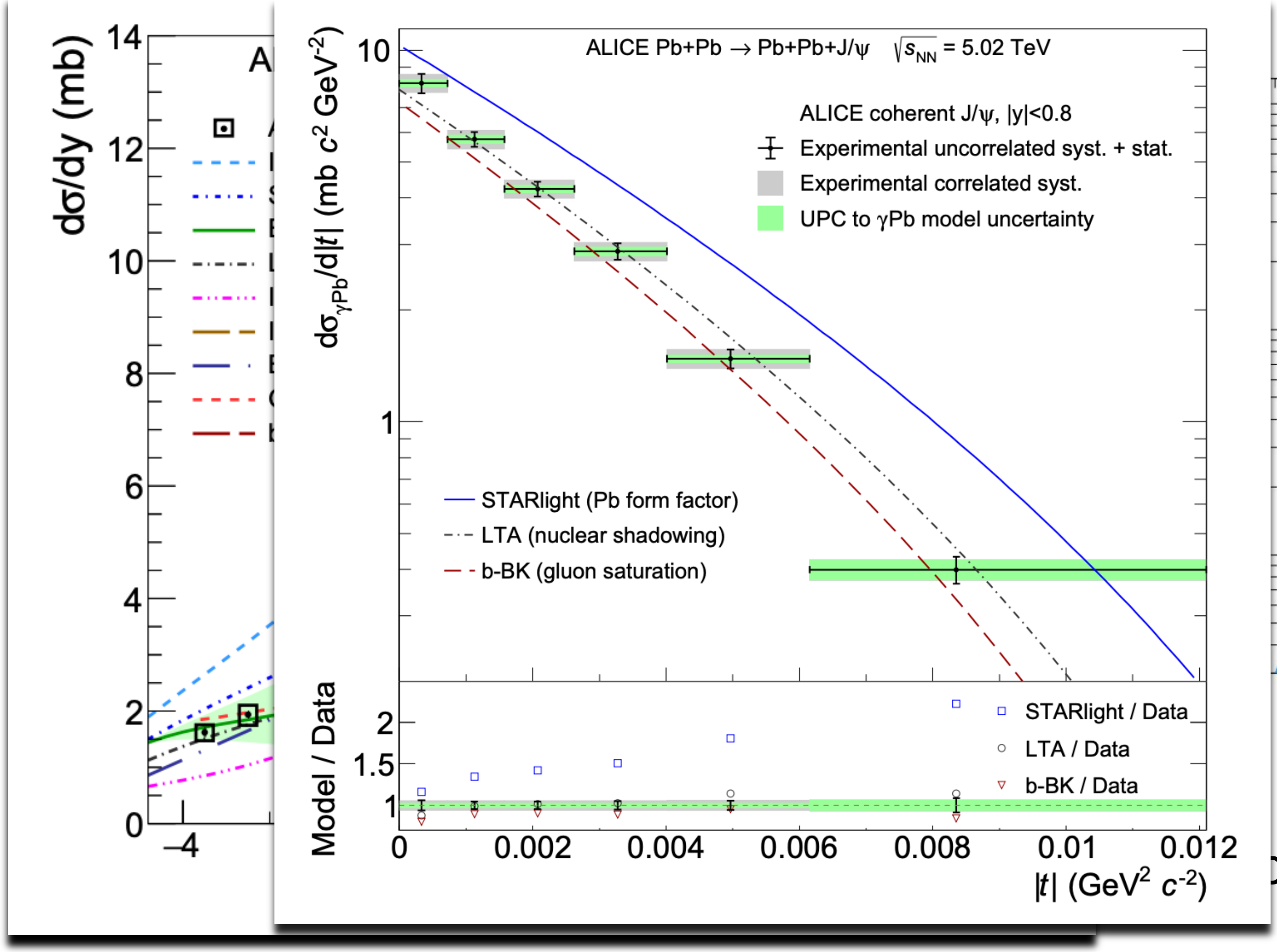

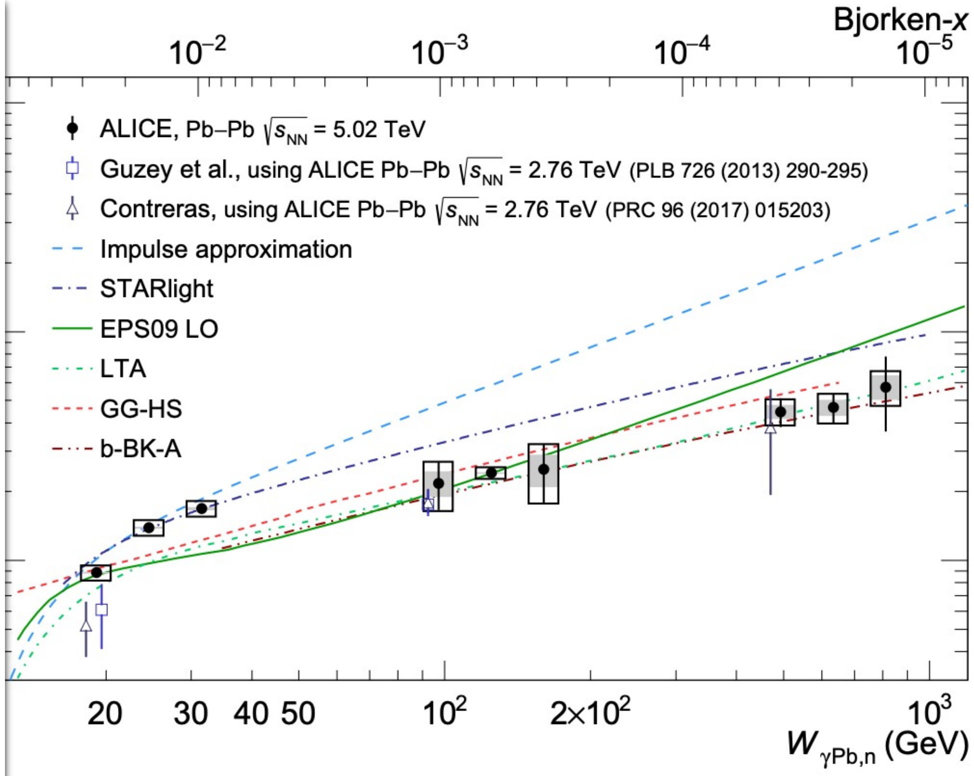

can somewhat describe the higher energies.

Most, if not all, data and model comparisons are like these

PRL 131 (2023) 262301

JHEP 10 (2023) 119

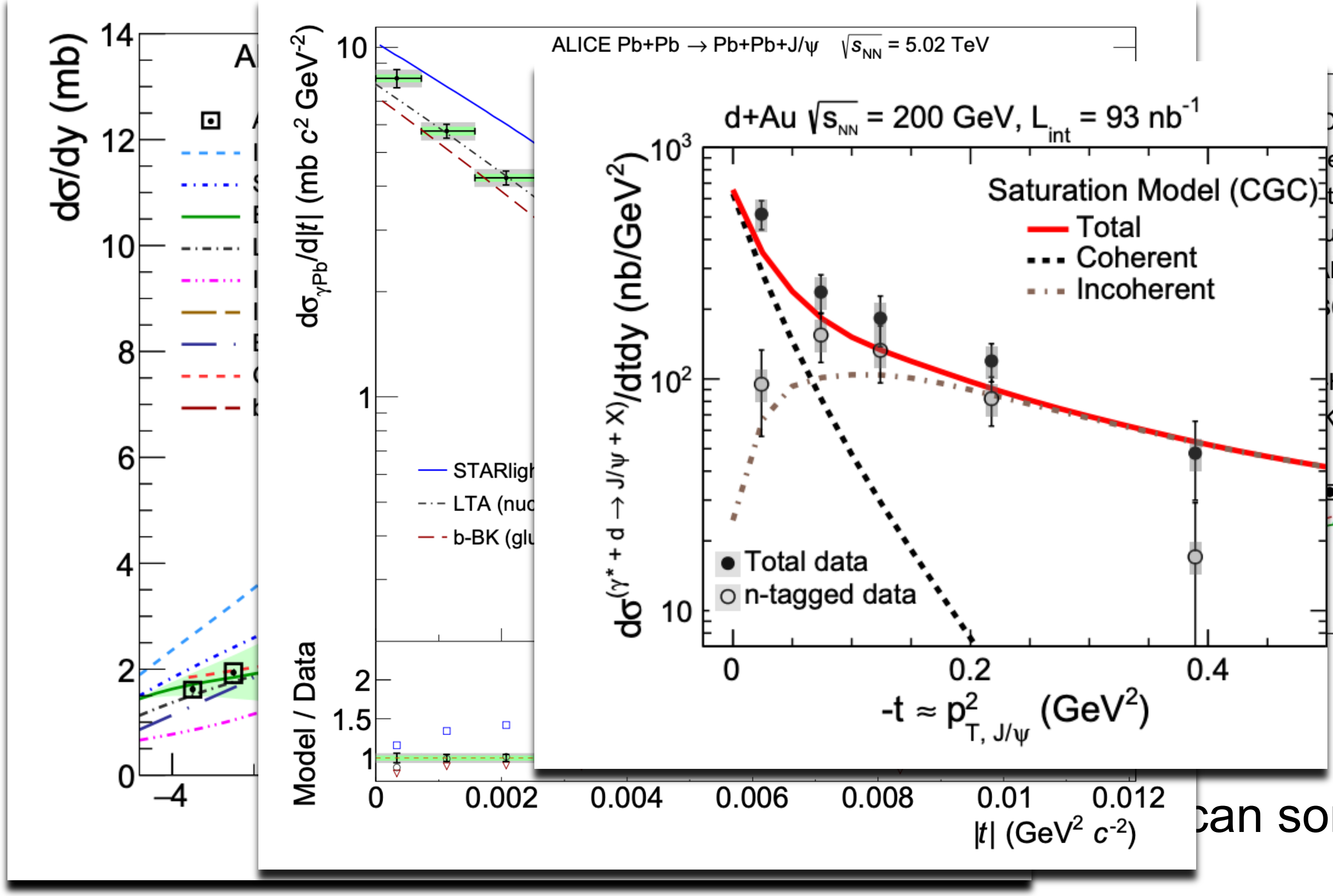

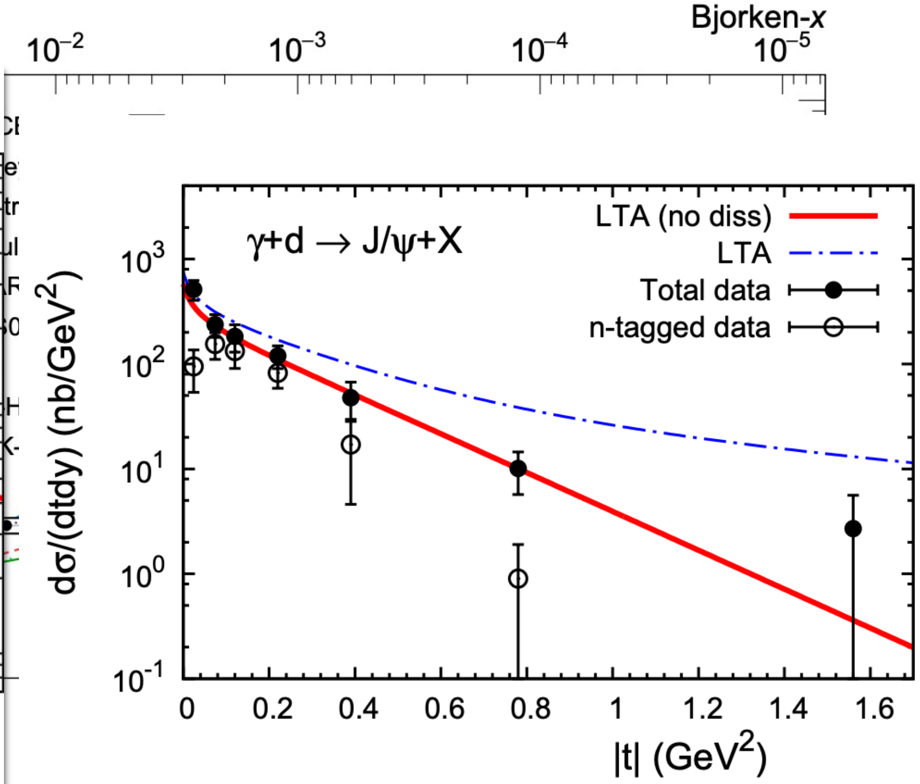

can somewhat describe the higher energies.

A. Double ratio in the quasi-classical approximation

1. *Elastic J/ψ and ρ production: heuristic estimates and numerical integration*

In Eq. (4) (or Eq. (17)), the dipole amplitude $N(\mathbf{r}, b, Y)$ describes the interaction of the quark-antiquark pair with the target nucleus. In processes where saturation effects are taken into account, one has to include multiple gluon exchanges between the $q\bar{q}$ pair and the nucleus. Including t-channel gluon exchanges to all orders in the GGM/MV model leads to the dipole amplitude [25]

$$N(\mathbf{r}, \mathbf{b}, Y) = 1 - \exp\left\{-\frac{r_\perp^2 Q_s^2(\mathbf{b})}{4} \ln \frac{1}{r_\perp \Lambda}\right\} \tag{22}$$

with the saturation scale Q_s given by

$$Q_s^2(\mathbf{b}) = 4\pi\alpha_s^2 \frac{C_F}{N_c} T(\mathbf{b}). \tag{23}$$

Here $T(\mathbf{b})$ is the nuclear profile (thickness) function,

$$T(\mathbf{b}) \equiv \int_{-\infty}^{\infty} dz\, \rho(\mathbf{b}, z), \tag{24}$$

where $\rho(\mathbf{b}, z)$ is the nucleon number density in the nucleus, Λ is the infrared (IR) cutoff, and C_F is the fundamental Casimir operator of SU(N_c). We should point out that the dipole amplitude given in Eq. (22) does not include small-x evolution: this is why $Q_s^2(\mathbf{b})$ here is independent of energy/rapidity Y, leading to similarly energy-independent dipole amplitude $N(\mathbf{r}, \mathbf{b}, Y)$ in Eq. (22).

Our goal now is to determine the dependence of the elastic VM production cross section on the atomic number A. After a closer inspection of Eq. (17), we see that the A-dependence is contained entirely in the $\mathbf{b}$-integral

$$\int d^2 b_\perp\, N(r_\perp, b_\perp, Y)\, N(r'_\perp, b_\perp, Y) \tag{25}$$

over the transverse area of the nucleus. This integral is hard to evaluate exactly analytically. Therefore, we have to make approximations for the dipole amplitude $N(\mathbf{r}, \mathbf{b}, Y)$ based on whether $r_\perp$ and $r'_\perp$ are larger or smaller than $1/Q_s(\mathbf{b})$, which corresponds to the dipole $r_\perp$ and/or the dipole $r'_\perp$ being inside or outside the saturation regime (see Fig. 5). Since the integrations over $r_\perp$ and $r'_\perp$ range over all positive values between 0 and ∞, we have three cases to consider: (i) $r_\perp, r'_\perp \ll 1/Q_s$, (ii) $r_\perp, r'_\perp \gtrsim 1/Q_s$, and (iii) $r_\perp \ll 1/Q_s, r'_\perp \gtrsim 1/Q_s$. The case when $r'_\perp \ll 1/Q_s, r_\perp \gtrsim 1/Q_s$ gives the same contribution as the case (iii), due to the $\mathbf{r} \leftrightarrow \mathbf{r}'$ symmetry of Eq. (17). As follows from Eq. (17), the dipole sized $r_\perp$ and $r'_\perp$ are controlled by the convolutions of the virtual photon and vector meson wave functions with the dipole size dependence of the amplitude N.

In these three regions we obtain different A-scaling, using the following arguments:

(i) $r_\perp, r'_\perp \ll 1/Q_s$: We approximate the dipole amplitude (22) outside the saturation region by expanding it to the lowest order in $r_\perp Q_s(\mathbf{b})$, such that

$$N(\mathbf{r}, \mathbf{b}, Y)\Big|_{r_\perp Q_s(\mathbf{b}) \ll 1} \approx \frac{r_\perp^2 Q_s^2(\mathbf{b})}{4} \ln \frac{1}{r_\perp \Lambda} \propto A^{1/3}, \tag{26a}$$

$$N(\mathbf{r}', \mathbf{b}, Y)\Big|_{r'_\perp Q_s(\mathbf{b}) \ll 1} \approx \frac{r'^2_\perp Q_s^2(\mathbf{b})}{4} \ln \frac{1}{r'_\perp \Lambda} \propto A^{1/3}, \tag{26b}$$

where the last proportionality follows from $Q_s^2(\mathbf{b}) \propto T(\mathbf{b}) \propto A^{1/3}$. Since the area integral scales as $\int d^2 b_\perp \sim A^{2/3}$, we conclude that

$$\int d^2 b_\perp\, N(\mathbf{r}, \mathbf{b}, Y)\, N(\mathbf{r}', \mathbf{b}, Y)\Big|_{r_\perp, r'_\perp \ll 1/Q_s} \propto A^{4/3}. \tag{27}$$

(ii) $r_\perp, r'_\perp \gtrsim 1/Q_s$: Inside the saturation region we approximate

$$N(\mathbf{r}, \mathbf{b}, Y)\Big|_{r_\perp Q_s(\mathbf{b}) \gtrsim 1} \approx N(\mathbf{r}', \mathbf{b}, Y)\Big|_{r'_\perp Q_s(\mathbf{b}) \gtrsim 1} \approx 1, \tag{28}$$

such that

$$\int d^2 b_\perp\, N(\mathbf{r}, \mathbf{b}, Y)\, N(\mathbf{r}', \mathbf{b}, Y)\Big|_{r_\perp, r'_\perp \gtrsim 1/Q_s} \propto A^{2/3}. \tag{29}$$

(iii) $r_\perp \ll 1/Q_s, r'_\perp \gtrsim 1/Q_s$ (or $r'_\perp \ll 1/Q_s, r_\perp \gtrsim 1/Q_s$): With one dipole being outside the saturation region, and another one being inside, we have

$$N(\mathbf{r}, \mathbf{b}, Y)\Big|_{r_\perp Q_s(\mathbf{b}) \ll 1} \approx \frac{r_\perp^2 Q_s^2}{4} \ln \frac{1}{r_\perp \Lambda}, \tag{30a}$$

$$N(\mathbf{r}', \mathbf{b}, Y)\Big|_{r'_\perp Q_s(\mathbf{b}) \gtrsim 1} \approx 1. \tag{30b}$$

This leads to

$$\int d^2 b_\perp\, N(\mathbf{r}, \mathbf{b}, Y)\, N(\mathbf{r}', \mathbf{b}, Y)\Big|_{r_\perp \ll 1/Q_s, r'_\perp \gtrsim 1/Q_s} \propto A. \tag{31}$$

Hence, we conclude that the elastic vector meson production cross section scales with A as a power of A,

$$\sigma_{\rm el}^{\gamma^* A \to V A} \propto A^\alpha, \tag{32}$$

with α between 2/3 and 4/3. The precise power of the scaling depends on the size of the vector meson: if the size of the vector meson is small (e.g., J/ψ), then the integral contribution would be dominated by region (i), and $\sigma_{\rm el}^{\gamma^* A \to J/\psi A} \propto A^{4/3}$; if the size of the vector meson is large (e.g., ρ), then the integral contribution would be dominated by region (iii), and $\sigma_{\rm el}^{\gamma^* A \to \rho A} \propto A^{2/3}$. Therefore, a transition from outside the saturation region into the saturation region should lead to the decrease of the (effective) power α defined in Eq. (32).

Notice that in Eq. (17) the integrand as a function of the dipole sizes $r_\perp$ and $r'_\perp$ is dominated by the Gaussian and the modified Bessel functions (which decrease exponentially at large $r_\perp$ and $r'_\perp$), so that the main contribution comes from the regions where $r_\perp, r'_\perp < \frac{1}{a_f}, R$. For J/ψ production in UPCs, where $Q^2 \approx 0$ and $a_f \approx m_c \approx 1.27$ GeV, this corresponds to $r_\perp, r'_\perp < \frac{1}{m_c} \approx 0.79$ GeV^{-1}. At relatively low x (x between 10^{-3} and 10^{-4}), the typical saturation scale for a gold nucleus ($A = 197$) is about $Q_s \approx 1$ GeV (see, e.g., Fig. 3.14 in [9]). We see that the $r_\perp, r'_\perp$-integrals in Eq. (17) are dominated by the non-saturated region (i), so that $\sigma^{\gamma^* A \to J/\psi A} \propto A^{4/3}$. However, these integrals do include contributions from larger $r_\perp, r'_\perp$, coming from the saturation region. Therefore, in an exact evaluation of Eq. (17), one may expect to see an A-scaling that is slightly slower than $A^{4/3}$, especially at the largest A when $1/Q_s$ starts to become comparable to the size of J/ψ and saturation effects start to settle in.